Development of a Measurement Container for the Time- and Frequency-Dependent Grid Impedance Identification on the 110 kV High Voltage Level

H. Langkowski, T. T. Do, M. Jordan and D. Schulz

Department of Electrical Power Systems
Helmut-Schmidt-University
Holstenhofweg 85, 22043 Hamburg (Germany)
phone:+49 6541 2905, fax:+49 6541 3083, e-mail: **Hauke.Langkowski@hsu-hh.de**

Abstract. In this contribution a novel measurement container is presented that allows to identify the grid impedances and their frequency characteristics on the 110 kV high voltage level. Thereby the capacity of a point of common coupling can be determined. The measurement results allow an improved grid planning and the dimensioning of necessary energy storages. The grid coupling of e.g. large wind parks can be assessed and suitable measures can be taken in order to optimize it. The measured frequency characteristic of the grid impedance can be used for an improved filter design and the control of the inverters within the context of the grid feedback and especially the harmonics.
The focus of this paper lies on the development of the novel measurement container. First the general measurement method is presented and then the extended method used for 110 kV high voltage grids. Afterwards the construction of the measurement container is presented. The main components of the measurement container are described in detail. Then the grid feedback on the high voltage level is introduced, the relationship with the grid impedance is analysed and possible improvements with the new prospective measurement results are outlined.

Key words: grid impedance, power quality, harmonics, grid integration, energy storage.

1. Introduction

The share of renewable energies of the electrical power supply in Germany will be further increasing in the future. The federal German government is supporting the planned increase up to a percentage of 80 % until 2050. Large wind parks are planned especially in the northern part of Germany and offshore in the North and Baltic Sea. In parallel an extensive grid expansion and the installation of new energy storages are required. In order to enable the efficient realization of this energy transition towards renewable energies an objective measurement of the current situation of the electrical power grid is necessary. Bottlenecks within the transmission system have to be identified. Deactivations and power reductions due to defiles in the electrical transmission system have to be avoided. Within the context of the increase of renewable energies the security of supply must not be lowered. In order to cope with the fluctuating energy generation energy storages have to be installed. These storages can close the gap between forecasted and actual generated power. Excessive energy can be absorbed and then be released later on.
In total the grid capacities and the locations of future energy storages have to be determined. The system-relevant parameter within this context is the grid impedance. The grid impedance is directly related to the capacity of a grid connection point in terms of the power at the fundamental frequency that can be obtained or fed-in and also in context of harmonics with the permissible grid feedback and the assessment of norms and technical guidelines [1], [2], [8], [9].
In the framework of this research project a transportable device is being developed that allows to measure the time- and frequency-dependent grid impedance of grid connection points directly on the 110 kV high voltage level. The objective measurement results can be used to determine the capacity of grid connection points and also to improve the planning and dimensioning of future wind parks especially within the context of the grid feedback. Distributed measurements at several points within the grid can then be used to dimension powers, capacities and locations of future large scale energy storage devices.

2. General Measurement Method

The general measurement method is based on the grid excitation with an ohmic high power and high voltage load resistor that is pulsed using power electronic, as shown in Fig. 1. The grid on the left side in Fig. 1 can be expressed with an ideal voltage source and the grid impedance. The frequency dependent grid impedance $\underline{\boldsymbol{Z}}_{\mathrm{G}}(\boldsymbol{\omega})$ contains an ohmic part $\boldsymbol{R}_{\mathrm{G}}(\boldsymbol{\omega})$ and an inductive part $\boldsymbol{L}_{\mathrm{G}}(\boldsymbol{\omega})$. Capacitive parts can mathematically be included in the inductance. The grid is excited using the power electronic switch and the load resistor, shown on the right side in Fig. 1.
The voltages and currents of the open loop phase ($\underline{\boldsymbol{V}}_{\boldsymbol{1}}$ and $\underline{\boldsymbol{I}}_{\boldsymbol{1}}$) and the excitation phase ($\underline{\boldsymbol{V}}_{\boldsymbol{2}}$ and $\underline{\boldsymbol{I}}_{\boldsymbol{2}}$) are measured with highly precise transducers. Then the FFT is used to obtain the frequency dependent grid impedances:

$$\underline{Z}_{\mathrm{G}}(\omega) = R_{\mathrm{G}}(\omega) + j\omega L_{\mathrm{G}}(\omega) = \frac{\underline{V}_1(\omega)-\underline{V}_2(\omega)}{\underline{I}_2(\omega)-\underline{I}_1(\omega)} = \frac{\Delta\underline{V}(\omega)}{-\Delta\underline{I}(\omega)} \quad (1)$$

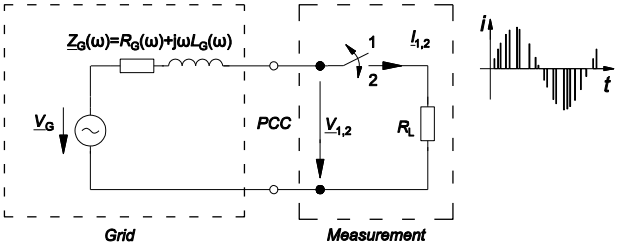

Fig. 1. General grid impedance measurement circuit

3. Grid Impedance Measurement in High Voltage Grids

On the 110 kV high voltage level there are in general three-wire systems installed. The grids are often wide-stretched. There are interconnections to other points so that the high voltage grids are meshed. 110 kV high voltage grids are often realized with large shares of overhead lines. Cables are mostly used in urban regions and within cities.
In Germany the 110 kV high voltage grids are mostly operated with compensated star points using earth-fault suppression coils or using low impedances in the connections between starpoints and earth. The starpoint treatment and the connection to the earth have a high influence on asymmetric failure currents e.g. during a single line to ground fault. The current value and also the prospective touch voltage are highly influenced by the starpoint treatment [11].
In order to identify the grid impedances of each conductor line in 110 kV high voltage grids several measurements of the different possible conductor loops can be used where only two outer conductors are taken at a time. The measurement method called "asynchronous switching" is applied [7].
The used measurement principle is presented in Fig. 2. In the equivalent circuit the grid on the left side is expressed with three ideal voltage sources and three grid impedances. The high voltage power electronic used within the measurement container that is being developed shown on the right side in Fig. 2, consists of a B6-diode-bridge and an IGBT. Each diode and the IGBT is built up of several devices connected in series due to the very high voltage. The power switch of the measurement container can be controlled so that each outer conductor can be switched separately and enables the conductor line selection required for the measurement method. A matrix operation finally leads to the individual grid impedances of each conductor line using the different loop impedances. Performing several measurements in succession allows to determine the time changes of the grid impedances.

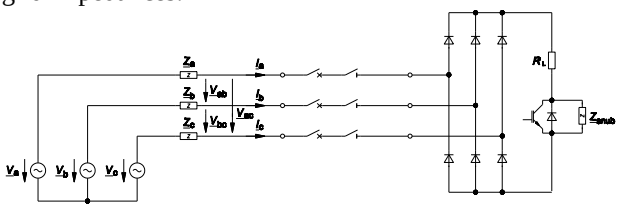

Fig. 2. Grid impedance measurement circuit on the 110 kV high voltage level

In the following a derivation based on the loop impedances will be described. In succession two outer conductor lines are used at a time to obtain in total three loop impedances. The load resistor is pulsed with the power electronic cyclically to two outer conductor lines at a time. Three linear independent equations can be generated:

$$\begin{aligned}
&\underline{V}_{1,\mathrm{ab}}(\mathrm{j}\omega) - \underline{I}_{2,\mathrm{a}}(\mathrm{j}\omega)\cdot\left(\underline{Z}_{\mathrm{a}}(\mathrm{j}\omega) + \underline{Z}_{\mathrm{b}}(\mathrm{j}\omega) + R_{\mathrm{L}}\right) = 0\\
&\underline{V}_{1,\mathrm{bc}}(\mathrm{j}\omega) - \underline{I}_{2,\mathrm{b}}(\mathrm{j}\omega)\cdot\left(\underline{Z}_{\mathrm{b}}(\mathrm{j}\omega) + \underline{Z}_{\mathrm{c}}(\mathrm{j}\omega) + R_{\mathrm{L}}\right) = 0\\
&\underline{V}_{1,\mathrm{ca}}(\mathrm{j}\omega) - \underline{I}_{2,\mathrm{c}}(\mathrm{j}\omega)\cdot\left(\underline{Z}_{\mathrm{c}}(\mathrm{j}\omega) + \underline{Z}_{\mathrm{a}}(\mathrm{j}\omega) + R_{\mathrm{L}}\right) = 0
\end{aligned} \tag{2}$$

The subscript 1 indicates that the IGBT switch is open and subscript 2 denotes that the IGBT switch is closed. Each time the occurring currents and voltages of the open and closed loop period are measured. During the closed loop periods when the load resistor is pulsed cyclically to the outer conductor lines "a" and "b", "b" and "c" and then "c" and "a" the following voltages $\underline{V}_{2,\mathrm{ab}}(\mathrm{j}\omega)$, $\underline{V}_{2,\mathrm{bc}}(\mathrm{j}\omega)$ and $\underline{V}_{2,\mathrm{ca}}(\mathrm{j}\omega)$ can be measured:

$$\begin{aligned}
\underline{V}_{2,\mathrm{ab}}(\mathrm{j}\omega) &= R_{\mathrm{L}}\cdot\underline{I}_{2,\mathrm{a}}(\mathrm{j}\omega)\\
\underline{V}_{2,\mathrm{bc}}(\mathrm{j}\omega) &= R_{\mathrm{L}}\cdot\underline{I}_{2,\mathrm{b}}(\mathrm{j}\omega)\\
\underline{V}_{2,\mathrm{ca}}(\mathrm{j}\omega) &= R_{\mathrm{L}}\cdot\underline{I}_{2,\mathrm{c}}(\mathrm{j}\omega)
\end{aligned} \tag{3}$$

Using the following voltage differences:

$$\begin{aligned}
\Delta\underline{V}_{\mathrm{ab}}(\mathrm{j}\omega) &= \underline{V}_{1,\mathrm{ab}}(\mathrm{j}\omega) - \underline{V}_{2,\mathrm{ab}}(\mathrm{j}\omega)\\
\Delta\underline{V}_{\mathrm{bc}}(\mathrm{j}\omega) &= \underline{V}_{1,\mathrm{bc}}(\mathrm{j}\omega) - \underline{V}_{2,\mathrm{bc}}(\mathrm{j}\omega)\\
\Delta\underline{V}_{\mathrm{ca}}(\mathrm{j}\omega) &= \underline{V}_{1,\mathrm{ca}}(\mathrm{j}\omega) - \underline{V}_{2,\mathrm{ca}}(\mathrm{j}\omega)
\end{aligned} \tag{4}$$

the first set of equations within this section can be reformulated to:

$$\begin{aligned}
\Delta\underline{V}_{\mathrm{ab}}(\mathrm{j}\omega) &= \underline{I}_{2,\mathrm{a}}(\mathrm{j}\omega)\cdot\left(\underline{Z}_{\mathrm{a}}(\mathrm{j}\omega) + \underline{Z}_{\mathrm{b}}(\mathrm{j}\omega)\right)\\
\Delta\underline{V}_{\mathrm{bc}}(\mathrm{j}\omega) &= \underline{I}_{2,\mathrm{b}}(\mathrm{j}\omega)\cdot\left(\underline{Z}_{\mathrm{b}}(\mathrm{j}\omega) + \underline{Z}_{\mathrm{c}}(\mathrm{j}\omega)\right)\\
\Delta\underline{V}_{\mathrm{ca}}(\mathrm{j}\omega) &= \underline{I}_{2,\mathrm{c}}(\mathrm{j}\omega)\cdot\left(\underline{Z}_{\mathrm{c}}(\mathrm{j}\omega) + \underline{Z}_{\mathrm{a}}(\mathrm{j}\omega)\right)
\end{aligned} \tag{5}$$

This leads to the three measured loop impedances:

$$\begin{aligned}
\underline{Z}_{\mathrm{ab}}(\mathrm{j}\omega) &= \underline{Z}_{\mathrm{a}}(\mathrm{j}\omega) + \underline{Z}_{\mathrm{b}}(\mathrm{j}\omega) = \frac{\Delta\underline{V}_{\mathrm{ab}}(\mathrm{j}\omega)}{\underline{I}_{2,\mathrm{a}}(\mathrm{j}\omega)}\\
\underline{Z}_{\mathrm{bc}}(\mathrm{j}\omega) &= \underline{Z}_{\mathrm{b}}(\mathrm{j}\omega) + \underline{Z}_{\mathrm{c}}(\mathrm{j}\omega) = \frac{\Delta\underline{V}_{\mathrm{bc}}(\mathrm{j}\omega)}{\underline{I}_{2,\mathrm{b}}(\mathrm{j}\omega)}\\
\underline{Z}_{\mathrm{ca}}(\mathrm{j}\omega) &= \underline{Z}_{\mathrm{c}}(\mathrm{j}\omega) + \underline{Z}_{\mathrm{a}}(\mathrm{j}\omega) = \frac{\Delta\underline{V}_{\mathrm{ca}}(\mathrm{j}\omega)}{\underline{I}_{2,\mathrm{c}}(\mathrm{j}\omega)}
\end{aligned} \tag{6}$$

The loop impedances can then be rearranged to the individual impedances of each outer conductor line:

$$\begin{aligned}
\underline{Z}_{\mathrm{a}}(\mathrm{j}\omega) &= \frac{1}{2}\cdot\left[\underline{Z}_{\mathrm{ab}}(\mathrm{j}\omega) - \underline{Z}_{\mathrm{bc}}(\mathrm{j}\omega) + \underline{Z}_{\mathrm{ca}}(\mathrm{j}\omega)\right]\\
\underline{Z}_{\mathrm{b}}(\mathrm{j}\omega) &= \frac{1}{2}\cdot\left[\underline{Z}_{\mathrm{ab}}(\mathrm{j}\omega) + \underline{Z}_{\mathrm{bc}}(\mathrm{j}\omega) - \underline{Z}_{\mathrm{ca}}(\mathrm{j}\omega)\right]\\
\underline{Z}_{\mathrm{c}}(\mathrm{j}\omega) &= \frac{1}{2}\cdot\left[-\underline{Z}_{\mathrm{ab}}(\mathrm{j}\omega) + \underline{Z}_{\mathrm{bc}}(\mathrm{j}\omega) + \underline{Z}_{\mathrm{ca}}(\mathrm{j}\omega)\right]
\end{aligned} \tag{7}$$

4. Measurement Container

There are two main components within the mobile grid impedance measurement container shown as a 3-D-CAD-model in Fig. 3. On the left side of the 40-feet long container in Fig. 3 there is in the outdoor part the gas-insulated power switch that is able to switch each conductor line individually. On the right side in Fig. 3 in the indoor part there is a special tank that contains the power electronic and the load resistor. The two main components are connected with a special relatively flexible high voltage cable. The tank is filled with about 10 m³ ester as insulation medium due to the high voltage. Ester additionally offers better environmental and safety aspects in comparison to oil. An air-insulated set-up of the measurement container cannot be realized with comparably small dimensions and does not allow a mobile device.

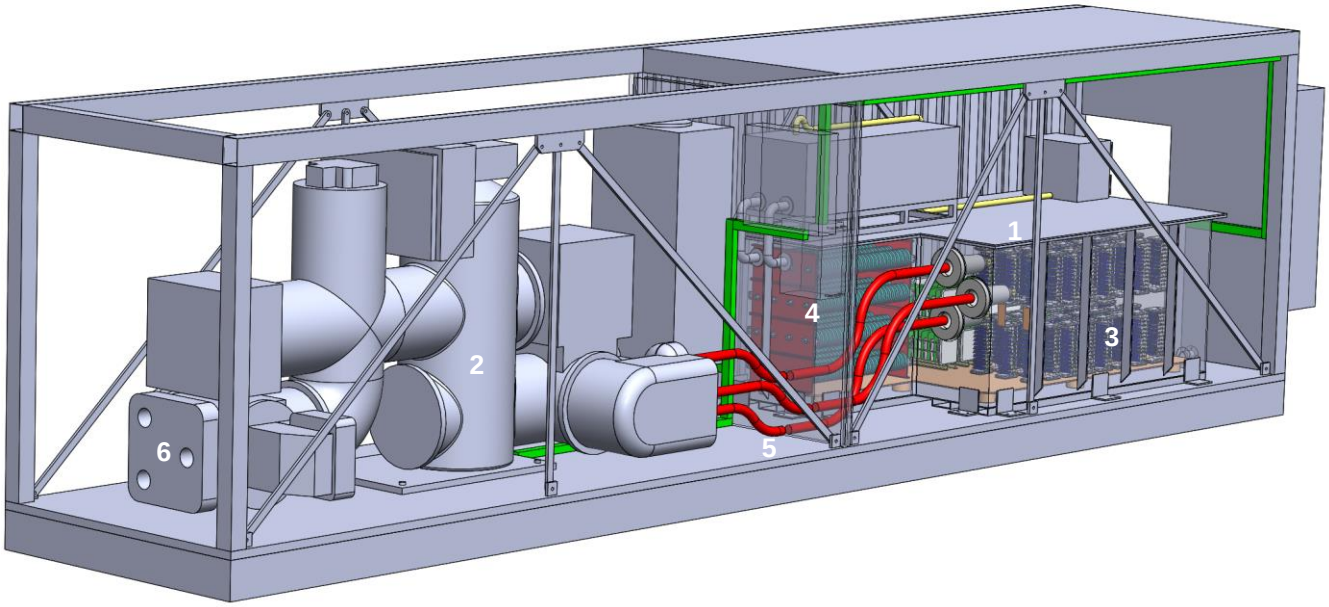

Fig. 3. 3-D-model of 110 kV grid impedance measurement container

1 - Tank filled with ester as isolation medium
2 - 110 kV power switch
3 - Power electronic
4 - High power resistors
5 - High voltage cable
6 - Grid connection

Due to the high weight and the outer dimensions a special heavy load transportation is required. Fig. 4 to Fig. 6 show the current status of the measurement container. The most important technical parameters of the measurement container are summarized in table 1.

Table 1: Technical parameters of 110 kV grid impedance measurement container

Parameter	**Value**
Nominal voltage (U_n)	110 kV
Dimensions	12,2 x 2,7 x 2,5 m
Rated current of power electronic (I_r)	200 A
Weight	~26 t

Fig. 4. Current construction status of the grid impedance measurement container

Fig. 5. Right side of the measurement container with indoor part where the ester filled tank will be installed

Fig. 6. Gas-insulated power switch located in the outdoor part of the measurement container

The rated current of the power electronic allows a peak grid excitation power of 22 MW. This high power is arising at the load resistor that contains a large number of

resistor discs out of a special ceramic material. The tank filled with ester features a very large heat capacity. The thermal energy is emitted to the air within the indoor part of the measurement container. Two large air conditioning systems with each having a cooling power of 15 kW are used to maintain a constant and not too high temperature within the tank. Several temperature sensors at different locations will be used for the supervision. The load resistor is pulsed using the power electronic, so the arising energy can be controlled with the pulse patterns applied to the power electronic.

A. Power Switch and High Voltage Cable

The SF6-insulated power switch facilitates the grid connection. The values from the local grid operator for the pressure relief in case of short-circuits are specified to a maximum short-circuit current of $I_k = 31{,}5\ kA$ at $T_k = 1\ s$. Due to the possible extreme energy in case of a short-circuit the power switch on the left side in Fig. 3 is located in the outdoor part of the measurement container.
There are current transducers for protective purposes installed within the power switch. Furthermore inductive voltage transducers and also highly precise and wide-band voltage transducers are installed within the power switch. Additionally highly precise Rogowski current transducers are mounted around the high voltage cables and are used for the measurements. Synchronous sampling of all measurement signals is necessary for the measurement method. The measurement and control system is located within the indoor part of the measurement container. Some technical parameters of the power switch are summarized in table 2.

Table 2: Technical parameters of 110 kV gas-insulated power switch

Parameter	Value
Manufacturer	Siemens
Type	8DN8
Rated voltage	123 kV
Rated lightning impulse voltage	550 kV
Rated operation current	1250 A
Rated short-time current	40 kA
Rated short-circuit duration	3 s
Weight of SF6 filling	102 kg
Total weight	4,7 t

The power switch is connected with the tank over a special relatively flexible high voltage cable using special high voltage plugs at both ends. The plugs and sockets from the company "*Pfisterer*" with type "HV-CONNEX Size 5-S" must not be exposed to any mechanical forces especially during the transportation. Therefore the cables are strutted at both ends in close distance to the plugs.
The flexible high voltage cable offers a very low bending radius. The technical parameters of the high voltage cable are listed in table 3. In fixed installation only $5 \cdot D$ with D being the outside diameter can be realized. There are rainproof bushings from the company "Roxtec" located within the wall between outdoor and indoor part of the measurement container. As shown in Fig. 3 a u-shaped design of the high voltage cables will be realized in order to cope with the mechanical forces. The deflection of the measurement container during lift up with a crane amounts to only about 1 mm along 1 m length of the container. The construction is realized with maximum torsional stiffness. There are several cross struts as shown in Fig. 3.

Table 3: Technical parameters of 110 kV cable

Parameter	Value
Manufacturer	Prysmian Group
Type	(N)TMCWOEU 132 (145) kV
Conductor	blank copper, fine wire class 5
Nominal cross section	240/85 mm²
Wire diameter	0,5 mm
Outside diameter	74,0 mm
Weight	7,6 kg/m
Resistance at 20°C	0,0801 Ω/km
Capacitance	0,153 µF/km
Nominal current (free in 30°C air and earthed at each end)	560 A
Rated short-time current (conductor/screen for T_k = 1 s)	34,7 kA/ 18.3 kA
Bending radius (fixed installation)	370 mm

B. Power Electronic

Each diode shown in Fig. 2 is consisting of 6 diode-stacks with each having 12 diodes in series. In total there are 432 diodes in the tank. The IGBT shown in Fig. 2 is built up of 15 stacks with each stack containing 6 IGBTs (90 in total). A 3-D-model of one diode stack and one IGBT stack are shown in Fig. 7. The gate drivers of the IGBTs are supplied directly out of the grid voltages. Active-clamping and metal-oxide varistors are used for overvoltage protection. The IGBTs are controlled over optical fiber cables. The control unit is located outside the tank.

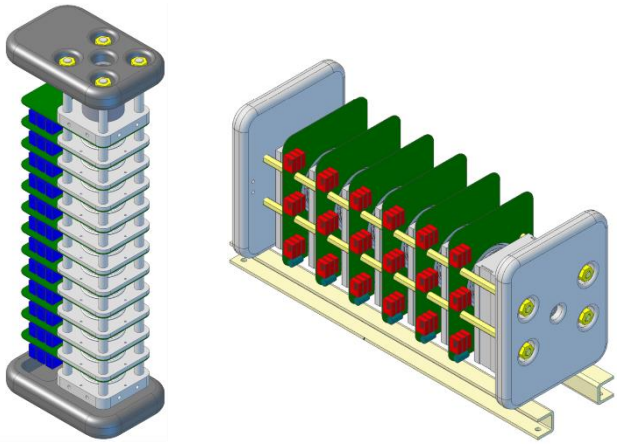

Fig. 7. 3-D-model of one diode stack (left side) and one IGBT stack (right side)

The power electronic is installed within the special tank and is completely surrounded by about 10 m³ ester. On the top of the tank there is a fluid reservoir for the ester. A vacuum pump will be used to ensure that no air bubbles are within the tank. The mechanical fixation of the power electronic is planned at the moment. In this construction

design certain distances must not be undercut to avoid partial discharges and voltage breakdowns. The set-up will first be tested with low voltages before the Ester is filled into the tank. Then also high voltages will be applied to test the set-up.

5. Grid feedback

A high quality of the electrical power system is given if the following factors can be found:

- constant frequency of 50 Hz (or 60 Hz in some countries)
- ideal sinusoidal voltage form
- high reliability

Long and short time outages of the power system can be regarded by measures concerning the security of supply. In the following the focus lies on the voltage quality that is in relation with the grid impedance. At a point of common coupling (PCC) the component of the grid impedance $|\underline{Z}_{\mathrm{PCC}}|$ at the fundamental frequency and the short-circuit power S_{kV} are directly related:

$$S_{\mathrm{kV}} = \frac{V_{\mathrm{PCC}}^2}{|\underline{Z}_{\mathrm{PCC}}|} \tag{8}$$

High short-circuit power meaning low grid impedance results in low voltage drops when connecting loads and also low voltage increase for the connection of generation units. In addition to the determination of grid capacities the measurement results of the grid impedance measurement can be used within the context of renewable energies and the resulting voltage form due to their power feed-in. The ideal voltage form can be further reduced by grid feedback like:

- harmonics, interharmonics and subharmonics
- voltage fluctuations (flicker)
- voltage asymmetries
- transients
- frequency variations
- voltage dips and overvoltages

The main sources and reasons are caused by nonlinear grid equipment and switching operations. The progressive use of power electronic in many loads but also in the inverters of renewable energies is supporting this trend. Wind energy converters (WEC) and photovoltaic power plants are using power electronic within the inverters to feed their power into the grid. Harmonic currents are produced that affect the power quality of the grid [9]. The statutory limits of the harmonic currents and also for the affected harmonic voltages must not be exceeded [1]. There are a number of possible negative consequences by harmonics:

- reduction of the efficiency
- destruction of isolations
- reduction of the life span
- overload in the neutral line (in low voltage grids)
- thermal stress
- failure or dysfunction of protection and measurement devices
- damping and distortion of signals (e.g. frequency remote control, power line communication)
- zero-crossing disturbances

This effect is increasing with growing installed power of renewable energies. The grid feedback can be assessed using the measured frequency characteristics of the grid impedances. Possible resonances in the frequency characteristics of the grid impedances can be identified.
Some selected limitation values of voltages and currents on the high voltage level are summarized in table 4. The harmonic voltage limitation values from the EN50160 are higher than the corresponding values specified in the guidelines for WEC in Germany (VDN-guideline [3]). In sections of the electrical power systems with no sensitive consumers and low background distortion within the context of harmonics the grid operator can permit higher limitation values.

Table 4: Limitation values for certain harmonics at 110 kV high voltage level ([3] and [6])

Order v	Iv [A/GVA] (acc. to [3])	Vv/Vn (acc. to [3])	Vv/Vn (acc. to [4])
5	2.6	0.25 %	5.0 %
7	3.75	0.5 %	4.0 %
11	2.4	0.5 %	3.0 %
13	1.6	0.4 %	2.5 %
17	0.92	0.3 %	tba.
19	0.70	0.25 %	tba.
23	0.46	0.2 %	tba.
25	0.32	0.15 %	tba.

If large wind parks are connected to the high-voltage level over HVDC-systems the harmonic emission of the total system must be specified up to a frequency of 10 kHz [3]. Additionally to the harmonic emission values the THD (total harmonic distortion) is used to evaluate the power quality of the WECs:

$$THD_{\mathrm{V}} = \frac{\sqrt{\sum_{i=2}^{40} V_{\mathrm{i}}^2}}{V_1} \tag{9}$$

On the medium-voltage level the THD_{V} must not increase to over 8 % [5]. On the high-voltage level there is no value specified in [3] and [4] for the THD_{V}. Furthermore there are also limitation values for the flicker produced by the WEC.

The limitation values of harmonic voltages and currents are based on the assumption that the grid impedance is consisting of an ohmic and an inductive part as described in section 2. In reality however there can be quite different frequency characteristics and resonance points due to capacitive elements. At these resonance points the limitation values can be exceeded by WECs and even instability can occur. Then the power has to be restricted or additional filters have to be installed. The design of grid-side filters can be improved using the knowledge of the grid impedance [10]. Also the internal control of the voltage and currents controllers used within the inverters can be adapted to the grid impedance avoiding possible power fluctuation and instability issues [6].

The harmonic propagation of WECs connected to the grid is illustrated in Fig. 8. The current of the WECs fed into the grid is affecting the grid voltages at the PCC. However there can also be an initial level harmonic pollution within the grid voltages before the WECs are active. The missing part of the assessment of the harmonic propagation are the impedances of the grid and also of the WEC. Both can be identified with the novel measurement container. Using the measured absolute values and the phase angles allows to conduct a correct calculation of the harmonic propagation.

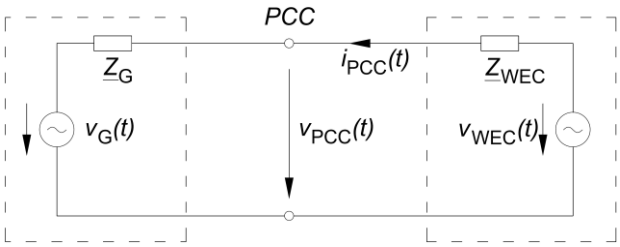

Fig. 8. Harmonic propagation of WEC at PCC

6. Conclusion

In this research project a novel measurement container is being developed that allows the identification of the time- and frequency-dependent grid impedances on the 110 kV high voltage level. Practical conclusions about the degree of capacity utilization can be made. The mobile grid impedance measurement container can be used to determine the capacity of grid connection points. At existing wind parks the determination of the remaining grid capacity for the connection of additional wind energy converters can be achieved. The grid expansion and installation of necessary energy storage devices can be planned and dimensioned based on the results. Additionally the grid feedback and propagation of harmonics caused by renewable energies can be assessed using the measurement results of the frequency characteristics of the grid impedances. Furthermore the measurement results can be used as an objective criterion at issues between the grid operators of the transmission and distribution grid and also the wind park operator.

In this contribution the development of the measurement container and its main components are presented. The general measurement method to identify the grid impedance and the extended method for 110 kV high voltage grids are described. The relationship of the grid impedance with the grid feedback of windparks is explained and some prospects for an improved grid integration of renewable energies based on the measurement results are outlined.

Acknowledgement

The project "*Development of a measurement device for the determination of the frequency dependent grid impedance on the high voltage level up to 110 kV for the assessment of the availability of grid capacities as a system parameter for the dimensioning of energy storages*" is funded by the German Ministry for the Economy and Energy under the support code 0325562. The two project partners "Stromnetz Hamburg GmbH" and "Astrol Electronic AG" are highly contributing with not only technical but also financial support.

References

[1] H. Langkowski, T. T. Do, and D. Schulz, "Grid Impedance Determination – Relevancy for Grid Integration of Renewable Energy Systems", IEEE IECON-09, Porto (2009).

[2] D. Schulz, Power Quality – Theory, Simulation, Measurement and Assessment (in German), VDE-Verlag, Offenbach (2004), ISBN 3-8007-2757-9.

[3] VDN, Technical Guideline for EEG Power Generation Plants at High and Highest Voltage Grid (in German), VDN, Berlin (2004).

[4] DIN EN50160, Characteristics of the Voltage in Public Electrical Power Supply networks, (2011).

[5] BDEW, "Technical Guideline for Power Generation Plants at Medium-Voltage Grid", (in German), BDEW, Berlin, 2008.

[6] M. Liserre, R. Teodorescu and F. Blaabjerg, "Stability of Photovoltaic and Wind Turbine Grid-Connected Inverters for a Large Set of Grid Impedance Values", IEEE Transactions on Power Electronics, Vol. 21, No. 1, Jan. 2006.

[7] T. T. Do T, S. Schostan, K.-D. Dettmann and D. Schulz, "Nonsinusoidal Power Caused by Measurements of Grid Impedances at Unbalanced Grid Voltages", IEEE, Lagow, Poland, 2008.

[8] M. Sumner, B. Palethorpe and D. W. P. Thomas, "Impedance Measurement for Improved Power Quality - Part 1: Measurement Technique", IEEE Transactions on Power Delivery, Vol. 19(3), 1457-1463, 2004.

[9] K. Yang, M. H. J. Bollen and M. Wahlberg, "A comparison study of Harmonic Emission Measurements in Four Windparks", IEEE-Power and Energy Society General Meeting, ISSN: 1944-9925, San Diego, USA, 2011.

[10] M. Liserre, F. Blaabjerg and S. Hansen, "Design and Control of an LCL-filter based Three-phase Active Rectifier", IEEE Transactions on Industry Applications, Vol. 41, ISSN: 0093-9994, Sept. 2005.

[11] K. Heuck, K.-D. Dettmann, and D. Schulz, "Elektrische Energieversorgung", Vieweg, 10th Edition, Wiesbaden, 2010.